



LAWRENCE  
LIVERMORE  
NATIONAL  
LABORATORY

UCRL-TR-225709

# Nuclear Car Wash sensitivity in varying thicknesses of wood and steel cargo

J.A. Church, D.R. Slaughter, S. Asztalos, P. Bilotto, M.-A. Descalle, J. Hall, D. Manatt, J. Mauger, E.B. Norman, D. Petersen, S. Prussin

October 31, 2006

## Disclaimer

---

This document was prepared as an account of work sponsored by an agency of the United States Government. Neither the United States Government nor the University of California nor any of their employees, makes any warranty, express or implied, or assumes any legal liability or responsibility for the accuracy, completeness, or usefulness of any information, apparatus, product, or process disclosed, or represents that its use would not infringe privately owned rights. Reference herein to any specific commercial product, process, or service by trade name, trademark, manufacturer, or otherwise, does not necessarily constitute or imply its endorsement, recommendation, or favoring by the United States Government or the University of California. The views and opinions of authors expressed herein do not necessarily state or reflect those of the United States Government or the University of California, and shall not be used for advertising or product endorsement purposes.

This work was performed under the auspices of the U.S. Department of Energy by University of California, Lawrence Livermore National Laboratory under Contract W-7405-Eng-48.

# Nuclear Car Wash sensitivity in varying thicknesses of wood and steel cargo

J.A. Church <sup>a</sup>, D.R. Slaughter <sup>a</sup>, S. Asztalos <sup>a</sup>, P. Biltoft <sup>a</sup>,  
M.-A. Descalle <sup>a</sup>, J. Hall <sup>a</sup>, T. Luu <sup>a</sup>, D. Manatt <sup>a</sup>, J. Mauger <sup>a</sup>,  
E.B. Norman <sup>a</sup>, D. Petersen <sup>b</sup> S. Prussin <sup>b</sup>

<sup>a</sup>*Lawrence Livermore National Laboratory, 7000 East Avenue, Livermore, CA  
94550*

<sup>b</sup>*Lawrence Berkeley National Laboratory, One Cyclotron Rd., Berkeley, CA  
94720*

---

## Abstract

The influence of incident neutron attenuation on signal strengths in the Nuclear Car Wash has been observed experimentally for both wood and steel-pipe mock cargos [1]. Measured decay curves are presented for  $\beta$ -delayed high-energy  $\gamma$ -rays and thermalized neutrons following neutron-induced fission of HEU through varying irradiation lengths. Error rates are extracted for delayed- $\gamma$  and delayed-n signals integrated to 30 seconds, assuming Gaussian distributions for the active background. The extrapolation to a field system of 1mA deuterium current and to a 5 kg sample size is discussed.

---

## 1 Introduction

In the fight against terrorism at our nation's ports, active cargo container interrogation can confirm the presence of fissile material in the assessment of a possible threat. At Lawrence Livermore National Laboratory, one such system 'the Nuclear Car Wash' [1–5] is currently undergoing feasibility testing. The system employs active neutron interrogation, using neutrons to induce fission, and then taking subsequent  $\beta$ -delayed high-energy  $\gamma$ -rays as the signal that fissile material has been stowed in the cargo. In some cases, the decay of delayed neutrons is used in conjunction with that of the delayed  $\gamma$ -rays as this signature. One goal for the system is to limit the scanning time per container to 1 minute while retaining 95% detection and 0.1% false alarm rates.

A system prototype has been set up to facilitate tests with hydrogenous and metallic cargos. Recent experiments designed to test the effects of incident

neutron attenuation show that the method is successful, and has the potential to play a major role in reducing the false alarm rates in any combined-method scanning apparatus that may be implemented at the seaports.

## 2 $\beta$ -delayed radiation signals fissile material

The Nuclear Car Wash uses  $\beta$ -delayed radiation to signal the presence of fissile material in cargo. It has been shown that after thermal-neutron induced fission,  $\beta$ -delayed  $\gamma$ -rays with  $E_\gamma \geq 3$  MeV are a unique signature for  $^{235}\text{U}$  and  $^{239}\text{Pu}$  [6]. Many of these fission products have half-lives ranging  $1 \text{ s} \leq t_{1/2} \leq 30 \text{ s}$  and also have high Q-values to  $\beta$ -decay [7]. This indicates that there is a chance for many decays within the 1 minute per scan goal, and that in these decays there is an equally important chance that a high-energy  $\gamma$ -ray will be emitted, and because of its energy, will escape full attenuation by the cargo. While the number of high energy  $\gamma$ -rays emitted by a particular fission product per fission may be small, the sum of these  $\gamma$ -rays over the wide mass distribution of fission products is large enough to consider. (For reference, 0.127 delayed  $\gamma$ -rays with energy above 3 MeV and 0.015 delayed neutrons are emitted per fission for thermal fission in  $^{235}\text{U}$  [7].) Their attenuation at  $E_\gamma \geq 3$  MeV is small even in thick cargos, smaller than attenuation at any other energy. Consequently, and because significant natural background  $\gamma$ -radiation falls below 2.6 MeV, this summed number of high-energy  $\beta$ -delayed  $\gamma$ -rays escaping the cargo becomes a workable signal for the presence of fissile material in thick cargo.

## 3 Experiment setup

The experiment setup (Fig. 1 and Fig. 2) consists of a broad spectrum 3-7 MeV neutron source, 8 large area plastic scintillators for  $\gamma$ -ray detection, and 14  $^3\text{He}$  tubes to count delayed neutrons. Smuggled nuclear material is represented with a sample of HEU ( $\text{U}_3\text{O}_8$ ) placed at various locations within  $0.55 \text{ g/cm}^3$  mock hydrogenous cargo (plywood), and separately in a  $0.6 \text{ g/cm}^3$  mock metallic cargo (steel pipes). The dimensions of the mock cargos are 229 cm x 122 cm x 178 cm.

Neutrons are produced in a  $d(d,n)$  reaction. A 4 MeV deuteron linac from Accsys Technologies (Pleasanton, CA) accelerates deuterons horizontally to 4 MeV. The deuteron beam direction is then bent 90 degrees upward by a high energy beam transport system and is delivered to the 1 atm, 60 cm long,  $\text{D}_2$  gas target cell at currents of 10-65  $\mu\text{A}$  nominally (100  $\mu\text{A}$  maximum). A 10

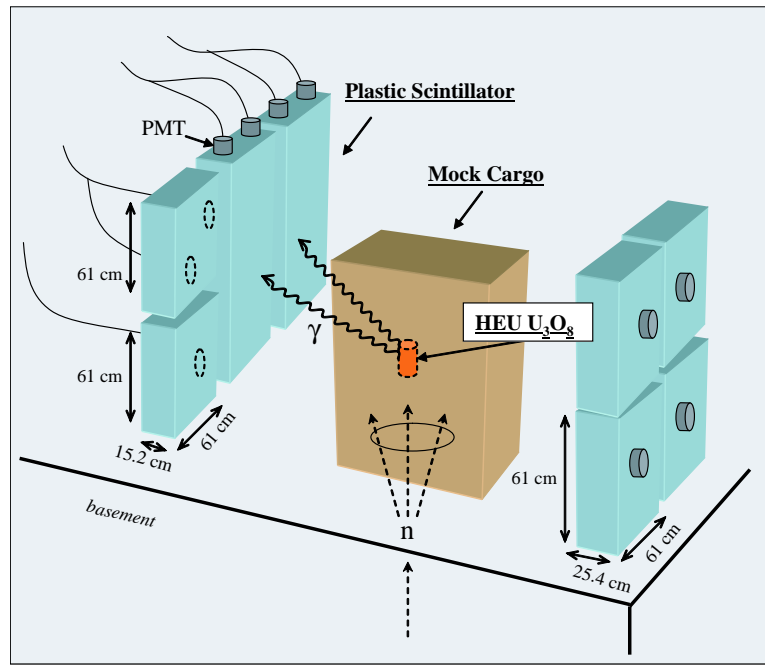


Fig. 1. The experiment setup for Nuclear Car Wash sensitivity tests.

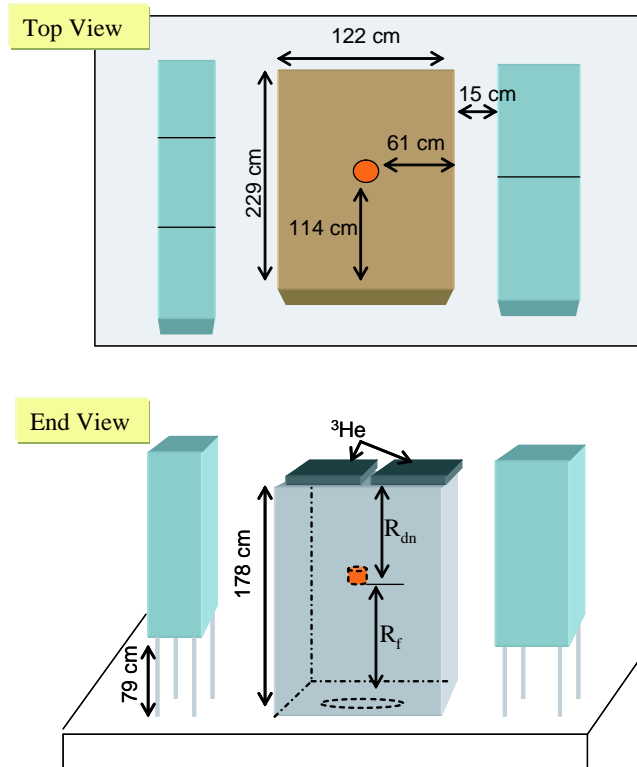


Fig. 2. Experiment dimensions.

$\mu\text{m}$  Mo window slows the beam to approximately 3.27 MeV upon entry into the cell where the incident deuterons are completely stopped.

Neutrons escape through the floor of the high bay laboratory via a polyethylene collimator with a 15 degree opening angle. Delayed  $\gamma$ -rays produced by the neutron-induced reactions are then detected in 4- 61 x 61 x 25.4 cm , 2- 61 x 61 x 15.2 cm and 2- 61 x 122 x 15.2 cm plastic scintillators which have energy resolutions of approximately 35% at 898 keV. The data presented here will represent the summed spectra for four 25.4 cm thick detectors. In addition to  $\gamma$ -ray detectors, 14  $^3\text{He}$  tubes were used to detect delayed neutrons during experiments with steel cargo. The  $^3\text{He}$  tubes are 5.08 cm in diameter, 91 cm long, are filled with 4 atm  $^3\text{He}$  and embedded in 10.16 cm thick polyethylene for moderation.

Experiments are performed by placing one of two samples of HEU ( $\text{U}_3\text{O}_8$ ), either 221.1 g or 376.5 g  $^{235}\text{U}$ , at varying depths within a mock cargo. The neutron generator is then cycled on for 30 seconds to induce fission and to allow sufficient build up of fission products with  $1\text{s} \leq t_{1/2} \leq 30\text{s}$ . Neutrons are then turned off, and gamma and neutron counters are allowed to count their respective  $\beta$ -delayed radiations for another 100 seconds.

## 4 $\gamma$ -ray background

System goals of 95% detection and 0.1% false alarm rates correspond to a signal strength  $5\sigma$  over 'active background,' defined as  $\gamma$ -rays counted after irradiation of the cargo only (no HEU). Variation in the active background must be understood in order to properly define the standard deviation ( $\sigma$ ). A preliminary study shown here investigates the dependence of the variation of the active background on deuterium current.

Figures 3 and 4 show the active background for different deuterium beam currents measured at the entrance of the  $\text{D}_2$  gas cell. The 'passive background,' taken without n-irradiation, has been subtracted. Data is displayed as a decay curve, the number of  $\gamma$ -rays depositing energies from 3 to 5 MeV taken in 1 s time bins plotted over 100 s after a single 30 s irradiation. Poisson  $2\sigma$  error bars are shown. The variation between curves of different beam current is significantly greater than  $\sqrt{N}$ , where N is the number of counts with energies from 3 to 5 MeV in a 1 s time bin. Using such a large variation would be overly conservative. The inset in Fig. 2 shows active backgrounds for the 3 highest beam currents after scaling to a beam current of 25  $\mu\text{A}$ . The passive background has been subtracted. The variation here is at least twice the Poisson standard deviation, and so, for the current work  $\sigma = 2\sqrt{N}$  will be used.

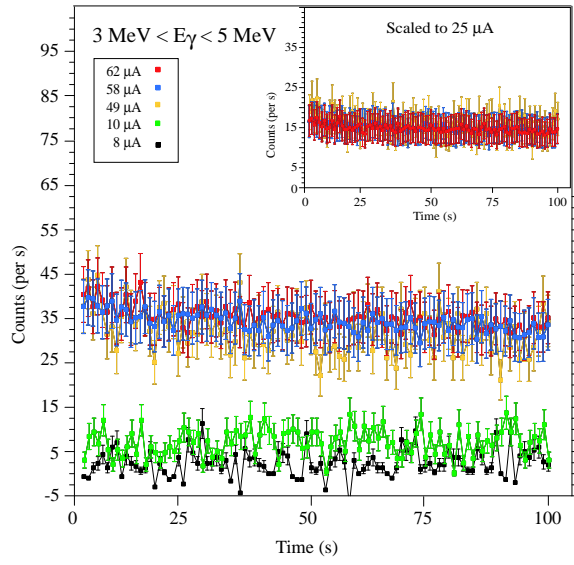


Fig. 3. Active  $\gamma$ -ray background for varying deuterium currents. The inset is scaled to  $25 \mu\text{A}$ .

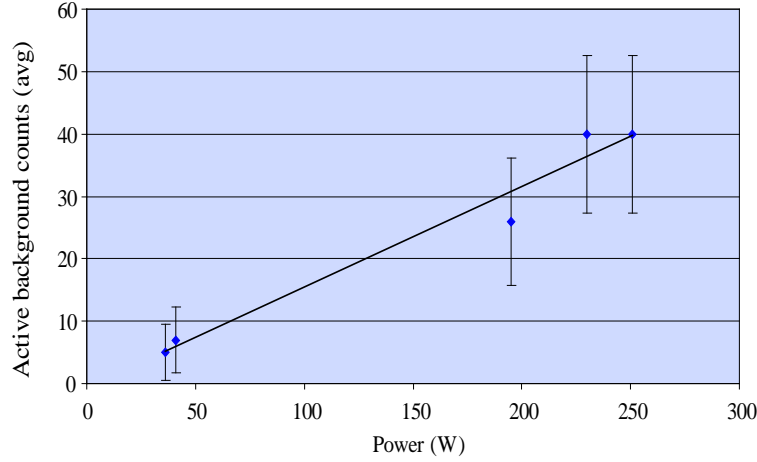


Fig. 4. Active  $\gamma$ -ray background for varying deuterium power into the  $\text{D}_2$  gas cell.

## 5 HEU in wood cargo

Feasibility tests were performed with HEU at various depths in plywood. Distances are shown in Fig. 2. The HEU sample within the wood was centered over the neutron aperture and the distance ( $R_f$ ) varied with respect to the floor to test the effects of neutron attenuation through the wood. The horizontal distance from the sample to the plastic scintillators remained the same at 61 cm.

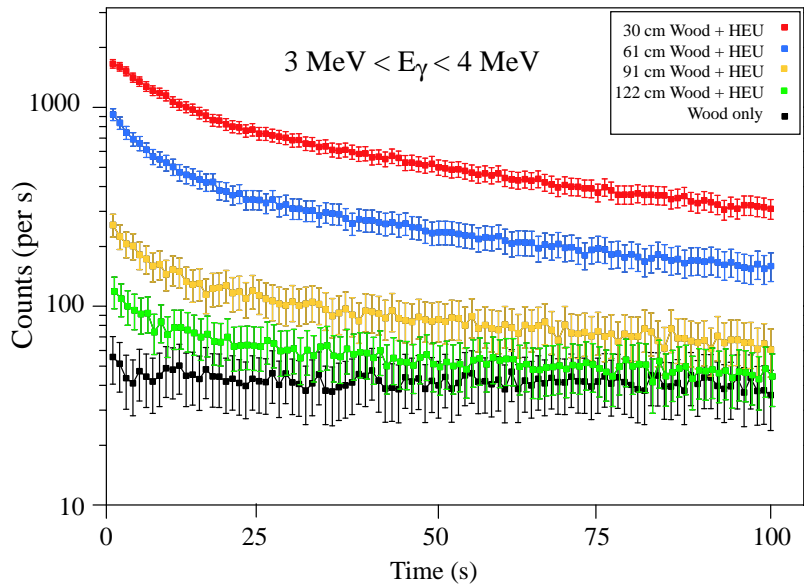


Fig. 5. Decay curves for HEU in wood after a single 30 s n irradiation. Distances correspond to  $R_f$ .

Decay curves for  $\gamma$ -rays depositing energies ( $E_\gamma$ ) between 3 and 4 MeV are shown in Fig. 4. The top two curves (red and blue) show the decay of fission products after n-irradiation of a 221 g sample of HEU  $U_3O_8$  through  $R_f = 30$  cm (red) and  $R_f = 61$  cm (blue). 3<sup>rd</sup> and 4<sup>th</sup> from the top are irradiations of 376 g HEU through  $R_f = 91$  cm (yellow) and  $R_f = 122$  cm (green). The bottom-most curve (black) is the active background, an irradiation of wood only, no HEU. Passive backgrounds have been subtracted, and all curves have been scaled to 25  $\mu$ A. Uncertainties shown are twice the Poisson standard deviation. At 30 s counting time, the 1 minute overall scan time limit is reached. Integrating from 1 to 31 s shows that, assuming  $\sigma = 2\sqrt{N}$ , signals for all 4 curves are at least  $5\sigma$  above active background, meeting goals for 95% detection probability and 0.1% false alarm rate. Integrated signal strengths are presented in Table 3.

## 6 HEU in steel cargo

Similar tests were also performed with HEU at various depths in a mock cargo of steel pipes ( $0.6 \text{ g/cm}^3$ ). The HEU sample within the steel was centered over the neutron aperture and the distance ( $R_f$ ) was varied with respect to the floor to test the effects of neutron attenuation and scattering through the steel. The horizontal distance from the sample to the plastic scintillators remained the same at 61 cm. Decay curves for  $\gamma$ -rays depositing energies ( $E_\gamma$ ) between 3 and 5 MeV are shown in Fig. 5. The top two curves (red and blue) show the

Table 1

Signals ( $N_{sig}$ ) and active backgrounds ( $N_{bkg}$ ) for HEU in mock cargo from the sum of four 10" detectors integrated 1 to 31 s following one 30 s irradiation, and scaled to 25  $\mu$ A beam current. Values for the standard deviation in the background signal,  $\sigma_{bkg}$ , include  $2\sqrt{N}$  statistical uncertainty, 10% uncertainty in the measurement of the beam current, and 5% uncertainty in the signal scaling. \*\* Indicates signals less than  $5\sigma$  ( $2\sqrt{N}$ ) above active background.

Signal	Cargo	$^{235}\text{U}$ (g)	$R_f$ (cm)	$N_{sig}$	$N_{bkg}$	$N_{sig} - N_{bkg}$	$\sigma_{bkg}$
Delayed $\gamma$	Wood	221.1	30	29217	1537	27679	186
$3 \leq E_\gamma \leq 4$ MeV		221.1	61	12715	1559	11156	189
		376.5	91	3717	1361	2356	167
		376.5	122	2306	1398	908	171
Delayed $\gamma$	Steel	376.5	46	7995	4775	3219	543
$3 \leq E_\gamma \leq 5$ MeV		376.5	76	6389	4232	2157	483
		376.5	122	6668	4775	1893	538
		376.5	1152	3963	3615	348**	415
Delayed neutron	Steel	376.5	46	1326	722	604	96
thermalized		376.5	76	1042	667	376	90
		376.5	122	1258	1117	141**	140
		376.5	1152	1466	667	800	90

decay of fission products after n-irradiation of a 376 g sample of HEU  $\text{U}_3\text{O}_8$  through  $R_f = 46$  cm (red) and  $R_f = 76$  cm (blue). The bottom-most curve (black) is the active background, an irradiation of steel only, no HEU. Passive backgrounds have been subtracted, and all curves have been scaled to 25  $\mu$ A.

Integrating from 1 to 31 s shows, assuming  $\sigma = 2\sqrt{N}$ , signals for both curves, and including  $R_f = 122$  cm of steel (not shown), are at least  $5\sigma$  above active background, meeting goals for 95% detection probability and 0.1% false alarm rate. Integrated signal strengths are presented in Table 3.

In order to measure the delayed neutron signal, 14  $^3\text{He}$  tubes were placed directly on top of the steel cargo. Their signals were read out during the 100 s  $\gamma$ -ray counting time. Bear in mind that because they were placed on top of the steel, steel thicknesses ( $R_{dn}$ ) causing attenuation for the delayed neutrons are  $R_{dn} = 178$  cm -  $R_f$ . The effect is evident in Table 3. Decay curves for delayed neutrons (thermalized counts in the  $^3\text{He}$  tubes) are shown in Fig. 6. The top two curves (red and blue) show the decay of fission products after n-irradiation of a 376 g sample of HEU  $\text{U}_3\text{O}_8$  through  $R_f = 152$  cm (red) and  $R_f = 76$  cm (blue). The bottom-most curve (black) is the active background, an irradiation

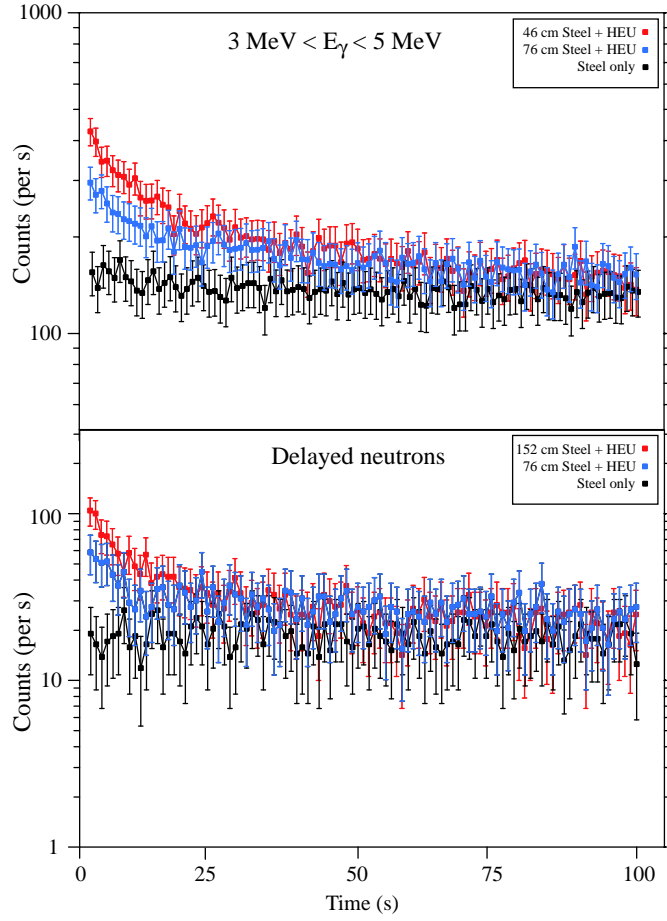


Fig. 6. Decay curves for HEU in steel after a single 30 s n irradiation. Delayed  $\gamma$ -rays are shown in the top panel and delayed neutrons in the bottom panel. Distances correspond to  $R_f$ .

of steel only, no HEU. Curves have been scaled to 25  $\mu$ A. Uncertainties shown are twice the Poisson standard deviation.

Integrating from 1 to 31 s shows, assuming  $\sigma = 2\sqrt{N}$ , signals for both curves, including 46 cm of steel (not shown), are at least  $5\sigma$  above active background, meeting goals for 95% detection probability and 0.1% false alarm rate. Integrated signal strengths are presented in Table 3.

## 7 Error rates

Error rates are examined using standard Gaussian probability distributions. Figure 7 is a graphical representation of sample background ( $B$ ) and signal-plus-background ( $S + B$ ) distributions with an alarm threshold level  $L$ . The

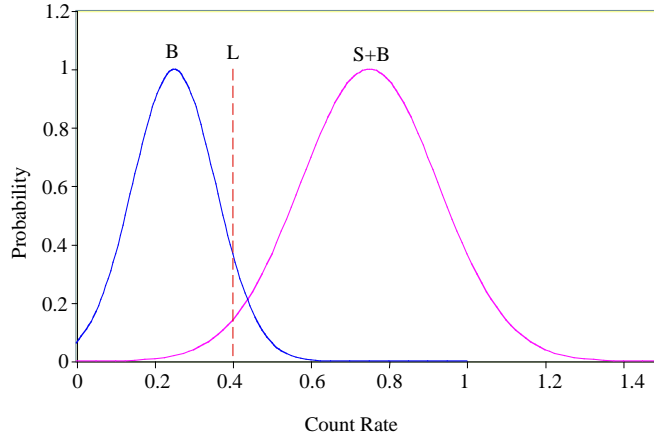


Fig. 7. Sample Gaussian distributions for the background ( $B$ ) and signal-plus-background ( $S + B$ ) with an alarm threshold level  $L$

probability for false alarm is given by:

$$P_{FA}(L, B, \sigma) = \int_L^{\infty} \frac{1}{\sqrt{2\pi}\sigma} e^{-0.5\left(\frac{x-B}{\sigma}\right)^2} dx = 0.5 \left[ 1 - \operatorname{erf} \left( \frac{(L-B)}{\sqrt{2}\sigma} \right) \right]. \quad (1)$$

Similarly, the expression for detection probability is:

$$\begin{aligned} P_D(L, S+B, \sigma) &= \int_L^{\infty} \frac{1}{\sqrt{2\pi}\sigma} e^{-0.5\left(\frac{x-(S+B)}{\sigma}\right)^2} dx \\ &= 0.5 \left[ 1 + \operatorname{erf} \left( \frac{(S+B-L)}{\sqrt{2}\sigma} \right) \right], \end{aligned} \quad (2)$$

where  $L$  represents the alarm threshold level above which detection is taken to be positive,  $B$  is the number of counts in the active background,  $S + B$  is the number of signal plus active background counts, and  $\sigma$  is the standard deviation in the number of counts in the active background.

Probability for detection,  $P(\text{Detection})$ , is plotted against the probability for false alarm,  $P(\text{FalseAlarm})$ , in Figure 8 (Receiver Operating Characteristic (ROC) curves) for delayed  $\gamma$  and delayed neutron signals in different thicknesses of both wood and steel cargos. The alarm threshold,  $L$ , is the independent variable. The standard deviation in the active background represents the  $2\sqrt{N}$  Poisson uncertainty, folded together with a 10% uncertainty in the value of the beam current, and 5% uncertainty in the scaling of the signal by the beam current (goodness-of-fit,  $R^2=0.96$ ) (See Fig. 4 and Table 1).

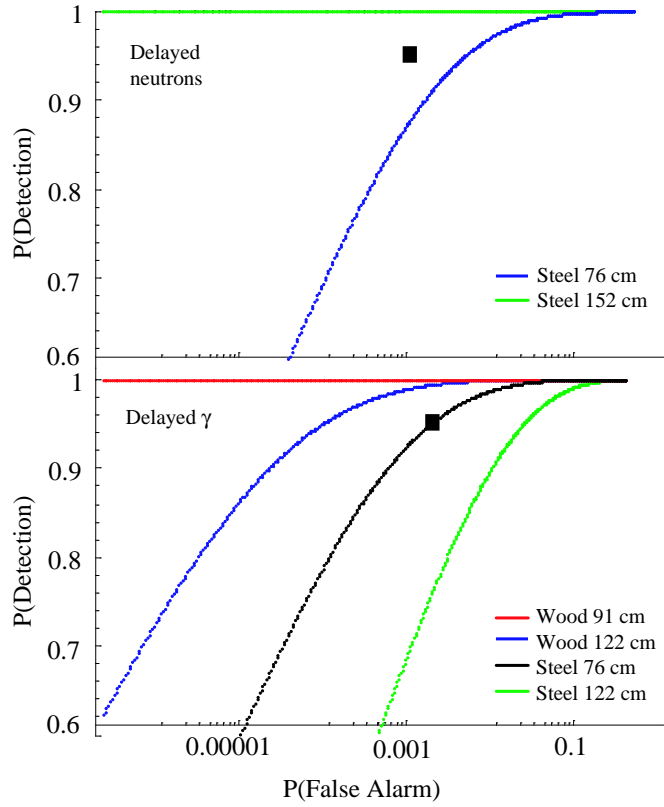


Fig. 8. Receiver Operating Characteristic (ROC) curves for both delayed neutron (top) and delayed  $\gamma$  signals in wood and steel cargos. The black square indicates 0.95 detection rate and 0.001 false alarm rate. Distances indicated refer to  $R_f$ . Source to  $^3\text{He}$  tube distances ( $R_{dn}$ ) varied inversely with  $R_f$ .

Even with these conservative estimates for the standard deviation, goals for 95% detection probability and 0.1% false alarm rates (represented by the black box in Figure 8) are met for thicknesses up to 122 cm in wood, and 76 cm in steel ( $0.6 \text{ g/cm}^3$ ) (both delayed  $\gamma$ -ray and delayed neutron signals).

## 8 Signal interferences

A brief search for signal interferences has been performed. Table 2 shows a few of the top candidates for interference in the  $\gamma$ -ray signal above 2 MeV, with half-lives under 30 s and at neutron energies below 7 MeV. The specific

Table 2

Top interference candidates.  $(A_\gamma/M)_{Rel}$  is specific activity relative to that for  $^{19}\text{F}(\text{n},\alpha)^{16}\text{N}$ , also explained in the text.

Reaction	Threshold (MeV)	$t_{1/2}$ (s)	$E_\gamma$ (MeV)	$(A_\gamma/M)_{Rel}$
$^{16}\text{O}(\text{n},\text{p})^{16}\text{N}$	10	7.13	6.128	-
$^{19}\text{F}(\text{n},\alpha)^{16}\text{N}$	1.6	7.13	6.128	1
$^{37}\text{Cl}(\text{n},\alpha)^{34}\text{P}$	1.6	12.43	2.127	$1.59 \times 10^{-5}$
$^{48}\text{Ca}(\text{n},\text{p})^{48}\text{K}$	0	6.8	3.831	$2.0 \times 10^{-6}$
$^{34}\text{S}(\text{n},\text{p})^{34}\text{P}$	4.72	12.43	2.127	$4.69 \times 10^{-6}$

activity defined as

$$\frac{A}{M} = \frac{0.693 N_0 \epsilon \sigma Y_\gamma}{A_0 T_{1/2}} |\phi_t|, \quad (3)$$

where  $M$  is the sample mass,  $N_0$  is Avogadro's number,  $\epsilon$  is the isotopic abundance,  $\sigma$  is the activation cross section,  $Y_\gamma$  is the  $\gamma$ -ray branching ratio,  $A_0$  is the atomic mass,  $T_{1/2}$  is the half-life, and  $\phi_t$  is the neutron fluence, was used to determine relative signal strengths [7]. The most significant interference comes from the  $\beta$ -decay of  $^{16}\text{N}$  to  $^{16}\text{O}$  emitting a 6.128 MeV  $\gamma$ -ray with a half life of 7.13 s. For neutrons with energies below 7 MeV, the major source of this interference is  $^{19}\text{F}(\text{n},\alpha)^{16}\text{N}$ . Specific activities relative to that for  $^{19}\text{F}(\text{n},\alpha)^{16}\text{N}$  ( $(A/M)_{Rel}$ ) are listed along with the interference material (Target), reaction, product, threshold, half life and major  $\gamma$ -ray energy.

An experimental test of several materials containing these isotopes revealed that these interference strengths are indeed fractions of that for  $^{19}\text{F}(\text{n},\alpha)^{16}\text{N}$ . 10 kg each of CaO, KCl, and  $(\text{NH}_4)_2\text{SO}_4$  were placed directly over the neutron aperture and irradiated separately for 30 seconds. For each material,  $\gamma$ -rays were counted with the plastic scintillators for 100 s. Decay curves constructed for energy windows corresponding to the most intense  $\gamma$ -ray expected for each of the isotopes show that for these 10 kg interference material samples, signals do not rise above active background. As a reference, 1.812 kg of Teflon ( $^{19}\text{F}$ ) was also irradiated, producing a signal at least  $5\sigma$  above active background for  $3 \text{ MeV} \leq E_\gamma \leq 5 \text{ MeV}$ . These results indicate that, except for  $^{19}\text{F}$ , there seems to be no other isotope in the chart of the nuclides likely to produce a significant interference to a  $\gamma$ -ray signal with energies above 3 MeV, decaying with a half-life between 1 and 30 seconds. While intense, the unique decay time and single peak high-energy  $\gamma$ -ray spectrum resulting from the  $^{16}\text{N}$   $\beta$ -decay is relatively easy to identify and it is feasible that the false positive it would cause can be suppressed.

## 9 Real-world projections

### 9.1 1mA deuterium current

In order to reduce the scan time per container in the Nuclear Car Wash, one possible action is to increase the overall neutron flux into the cargo while reducing irradiation time. The top portion of Table 3 presents extrapolations from our experimental observations scaled from a 25  $\mu$ A d-intensity and 30 s irradiation-time to a 1 mA deuterium current. The linear scaling factor was obtained empirically from measurements at different deuteron intensities (see Fig. 4). This simple scaling results in a factor of 40 increase in both signal and background for a single 30 second irradiation, and 30 s counting period for the 1 mA current. Assuming a linear dependence of the signal on irradiation time as well, for a 1 mA deuterium current, the signal would then increase by a factor of 6.5 when the irradiation time is reduced to 5 seconds.

### 9.2 5 kg HEU

Similarly, scaling can be done to extrapolate to a 5 kg HEU sample. In this case, Monte Carlo calculations were used, and the results are listed in Table 3 [5]. The calculations were performed for spheres of HEU placed in the center of the mock wood cargo ( $R_f=89$  cm), assuming 30 s irradiation followed by 100 s counting periods.  $\gamma$ -rays with  $E_\gamma \geq 3$  MeV were counted over one 122 x 61 x 15 cm detector. While attenuation in the cargo and the sample were taken into account, detector efficiency considerations were omitted for the calculation. Increasing the mass by a factor of 4 from 500 g actually results in a decrease in the number of  $\gamma$ -rays due to self-attenuation in the sample. Even doubling the mass from 500 g to 1 kg results in only a 5% increase in the number of delayed  $\gamma$ -rays with energies above 3 MeV.

## 10 Conclusion

We have shown experimentally that after n-induced fission,  $\beta$ -delayed radiation is indeed a unique signature for fissile material hidden in very thick wood and steel test cargos. For  $E_n \leq 7$  MeV, Nuclear Car Wash feasibility experiments show a clear delayed  $\gamma$ -ray signal  $5\sigma$  above background when incident neutrons are attenuated through up to 122 cm 0.55 g/cm<sup>3</sup> plywood or 122 cm 0.6 g/cm<sup>3</sup> steel, and a clear delayed neutron signal in steel,  $5\sigma$  above background where  $\sigma = 2\sqrt{N}$ . Using a more conservative value for the standard

Table 3

Scaled signals ( $N_{sig}^*$ ) and active backgrounds ( $N_{bkg}^*$ ) for HEU in mock wood cargo. Signal ( $N_{sig}^*$ ) and background counts ( $N_{bkg}^*$ ) measured in the sum of four 10"-thick detectors and scaled for deuterium currents of 25  $\mu$ A and 1 mA are shown in the top part of the table. The data was obtained by counting for 30 seconds following a single 30 s irradiation. Monte Carlo calculations (COG) [5] are listed in the bottom portion. Number of fissions ( $N_{(n,f)}$ ) and number of  $\gamma$ -rays reaching the face of one 6"-thick detector ( $N_\gamma$ ) are listed for deuterium currents of 25  $\mu$ A and 1 mA, gathered over 100s. Calculated number of  $\gamma$ -rays have not been corrected for the response function of the detector.

Measurement			25 $\mu$ A		1 mA	
Signal	$R_f$ (cm)	$^{235}\text{U}$ (g)	$N_{sig}^*$	$N_{bkg}^*$	$N_{sig}^*$	$N_{bkg}^*$
4- 10" detectors	61	221	12715	1559	5.09x10 <sup>5</sup>	6.24x10 <sup>4</sup>
$3 \leq E_\gamma \leq 4$ MeV	91	376	3717	1361	1.49x10 <sup>5</sup>	5.44x10 <sup>4</sup>

Calculation						
Signal	$R_f$ (cm)	$^{235}\text{U}$ (g)	$N_{(n,f)}$	$N_\gamma$	$N_{(n,f)}$	$N_\gamma$
One 6" detector	89	500	6.14x10 <sup>6</sup>	186	2.46x10 <sup>8</sup>	7.43x10 <sup>3</sup>
$E_\gamma \geq 3\text{MeV}$	89	1000	1.04x10 <sup>7</sup>	195	4.14x10 <sup>8</sup>	7.80x10 <sup>3</sup>
	89	2000	1.75 x10 <sup>7</sup>	76	7.00x10 <sup>8</sup>	3.04x10 <sup>3</sup>
	89	5000	3.96 x10 <sup>7</sup>	62	1.59x10 <sup>9</sup>	2.50x10 <sup>3</sup>

deviation in the background which includes uncertainties due to the measurement of the beam current and scaling of the signal, goals for 0.95 detection rate, and 0.001 false alarm rate using delayed  $\gamma$ -rays are reached for thicknesses through 122 cm wood and 76 cm steel pipe cargo. Similar success is found in our preliminary delayed-n measurements. Brief studies indicate that  $\gamma$ -ray interferences above 3 MeV resulting from species with half-lives below 30 s can be considered negligible except in the case of  $^{19}\text{F}(n,\alpha)^{16}\text{N}$ . In order to make the most accurate measurement of the false alarm rates for the Nuclear Car Wash, it will be necessary to perform a more detailed investigation into the variation and composition of the active background for both static and moving cargo scenarios. Our sensitivity study has made strong indications that the Nuclear Car Wash is a successful method for sniffing out fissionable material in thick cargo and will become even more robust with the addition of a detailed study of background variations.

This work was performed under the auspices of the United States Department of Energy by the University of California, Lawrence Livermore National Laboratory contract number W-7405-Eng-4, UCRL-TR-225709.

## References

- [1] J.A. Church *et al.*, Nucl. Instr. and Meth. **A**, CAARI proceedings (2006).
- [2] D.R. Slaughter *et al.*, Nucl. Instr. and Meth. **B 241**, 777 (2005).
- [3] D.R. Slaughter *et al.*, LLNL UCRL-ID 155315.
- [4] J. Pruet *et al.*, Journal of Appl. Physics 97, 94908 (2005).
- [5] J. Hall *et al.*, Nucl. Instr. and Meth. **A**, CAARI proceedings (2006).
- [6] E.B. Norman, *et al.*, Nucl. Instr. and Meth. **A 521**, 608 (2004).
- [7] National Nuclear Data Center, *www.nndc.bnl.gov*.